Volume 241, number 1,2, 239–245 FEB 06564 December 1988

Electron microscopy and image analysis of the multicatalytic proteinase

W. Baumeister, B. Dahlmann+, R. Hegerl, F. Kopp+, L. Kuehn+ and G. Pfeifer

Max-Planck-Institut für Biochemie, D-8033 Martinsried and +*Diabetes-Forschungsinstitut an der Unversität Düsseldorf, Auf'm Hennekamp 65, D-4 Düsseldorf 1, FRG*

Received 19 September 1988; revised version received 18 October 1988

On electron micrographs, negatively stained multicatalytic proteinase molecules are viewed end-on (ring shaped) or side-on (rectangular shaped). For aurothioglucose, ammonium molybdate- and phosphotungstate-stained molecules, the dimensions measured are consistent. In contrast, uranyl acetate-staining reveals ring-shaped particles which vary in diameter between 12 and 16 nm. This is due to a partial collapse and substantial flattening of the structure. Digital image analysis of side-on views of the particles reveals a tripartite, reel-shaped structure. Within the ring-like, end-on projections of ammonium molybdate-stained molecules six local centres of mass can be discerned; their position appears to depart, however, from a true six-fold symmetry.

Electron microscopy; Image analysis; Multicatalytic proteinase; Negative staining

1. INTRODUCTION

A neutral proteinase has been identified in a variety of eukaryotic cells and has been designated 'multicatalytic proteinase' (MCP) since it appears to contain more than one active site for catalysis of peptide-bond cleavage [1–3]. The latent enzyme which can be activated by SDS and fatty acids [1,4,5], by phospholipids [6] as well as by polylysine [3] is localized in the cytoplasm [3], in the cell nucleus [7] or in both compartments [8].

The enzyme purified from rat skeletal muscle has a molecular mass of 650 kDa [2]. A 19 S ribonucleoprotein (RNP) with a similar subunit pattern has been identified in a number of eukaryotic cells as reviewed in [9]. It has recently been shown that the MCP and the 19 S RNP share antigenic determinants, contain an RNA moiety and are both able to catalyze peptide-bond cleavage [8,10]. In addition, both particles have a common, characteristic morphology [10].

Contrary to other investigators who considered the molecule to be ring or disk shaped [11–15], we demonstrated by shadow-casting experiments with the freeze-dried molecule that it is four stacked rings or disks which give the typical cylinder-like shape of the high-molecular-mass proteinase [16]. Similarly, the 22 S particle of *Xenopus laevis* has been found to exhibit a cylinder shape [17]. To obtain further insight into the molecular architecture of this high-molecular-mass proteinase, we performed 2D image analysis of electron micrographs of the negatively stained muscle enzyme.

Correspondence address: W. Baumeister, Max-Planck-Institut für Biochemie, D-8033 Martinsried, FRG

2. MATERIALS AND METHODS

The multicatalytic proteinase was isolated from pooled rat skeletal muscles and purified as described previously [2]. For electron microscopy the enzyme was diluted with 20 mM Tris-HCl/1 mM EDTA/1 mM NaN_3/0.1% (v/v) β-mercaptoethanol, pH 7.5. For negative staining, carbon film coated grids were used which had been rendered hydrophilic by a thirty second exposure to a glow discharge in a plasma cleaner (Harrick Scientific Corporation, New York). Samples were stained with 1% (w/v, pH 4.1) uranyl acetate (UA), 2% (w/v, pH 7.2) sodium phosphotungstate (NaPT) or 2% (w/v, pH 7.5) ammonium molybdate (AM), or 3% (w/v) aurothioglucose (ATG).

Electron micrographs were recorded with a Philips EM 420

Published by Elsevier Science Publishers B.V. (Biomedical Division)
00145793/88/$3.50

at a (nominal) magnification of 49000 ×. Since care was taken not to preirradiate specimen areas to be imaged the total dose did not exceed 4000 e-/nm^2. All images were taken at room temperature, except for the ammonium molybdate stained preparation where, in addition, images were recorded at liquid nitrogen temperature (using a Gatan cryoholder) in order to minimize mass loss.

Suitable areas of the micrographs were densitometered with a step size of 20 μm, corresponding to 0.41 nm at the specimen level. Individual particles were selected interactively from the digitized micrographs using a Metheus Omega 445 rastergraphics display system. From each of the different preparations subjected to a detailed image analysis a total of 300 to 900 molecular images were selected. The molecular images were aligned with respect to translation and orientation using correlation techniques. An arbitrarily chosen reference was used

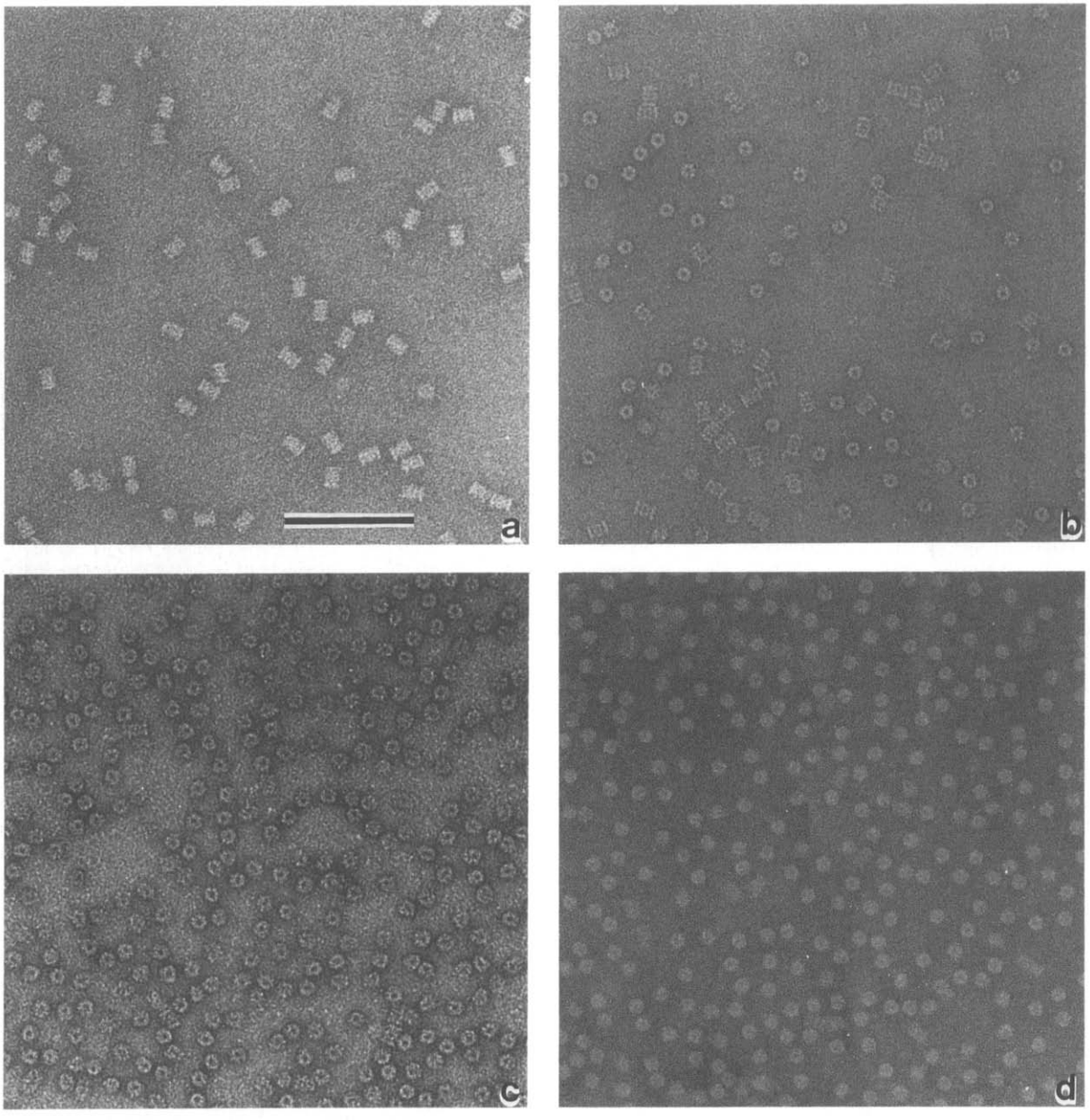

Fig.1. MCP particles negatively stained with (a) sodium phosphotungstate, (b) ammonium molybdate, (c) uranyl acetate, and (d) aurothioglucose. In (a) all particles are viewed 'side-on', in (c,d) all particles are viewed 'end-on'. Bar, 100 nm.

for the first correlation averaging cycle; the average resulting from it was then used as a reference in a refinement pass. The procedure included the application of appropriate masks to suppress peripheric background. In order to detect inter-image structural variations the aligned images were subjected to a classification procedure based on an eigenvector-eigenvalue data analysis [18]. All computations were performed using the EM [19] and Semper [20] programme systems.

3. RESULTS

Two distinct populations of molecular images can clearly be recognized on the electron micrographs: ring shaped and rectangular structures, the latter with an axial ratio of approx. 1 to 1.4. These two views can obviously be related to each other assuming that they represent either end-on or side-on projections of a cylindrically shaped particle. Very striking is the preponderance of either of the two projections in a given preparation: samples negatively stained with uranyl acetate or aurothioglucose (fig.1c,d) show predominantly the end-on views, while we find almost exclusively side-on views when sodium phosphatungstate is used as a negative stain (fig.1a). Only in preparations stained with ammonium molybdate are the two views found in about equal proportions (fig.1b).

Also the apparent dimensions of the MCP particles are subject to stain-specific variations (see table 1). Side-on views of particles embedded in NaPT appear slightly larger than those embedded in AM. Characteristic of UA stained preparations is a rather large variation in the diameter of end-on views. On a single grid we may find smooth transitions between areas with 12 nm particles and areas with particle diameters up to 16 nm; concomitant with this change in diameter, the central stain filled pit often moves towards the periphery of the particles, which is a further indication of a collapse of the structure (fig.2). Particles embedded in ATG, a 'low-contrast' negative stain, which is supposed to provide a particularly good preservation of proteins, are typically 12 nm in diameter (see table 1).

On unprocessed electron micrographs the side-on views of the MCP particles show four cross-striations arranged parallel to the short axes of the rectangles. Assuming that the MCP particles are cylinder shaped, one could therefore envisage them

Table 1

Apparent dimensions of MCP in different negative stains

Negative stain	Side-on views of rectangle		Diameter of rings (end-on views)
	Length	Width	
AM[a]	15 nm	11 nm	11 nm
PTA	16 nm	12 nm	–
UA	–	–	12–16 nm
ATG	–	–	12 nm

[a] Dimensions of MCP images recorded at room and LN_2 temperature, respectively, are identical

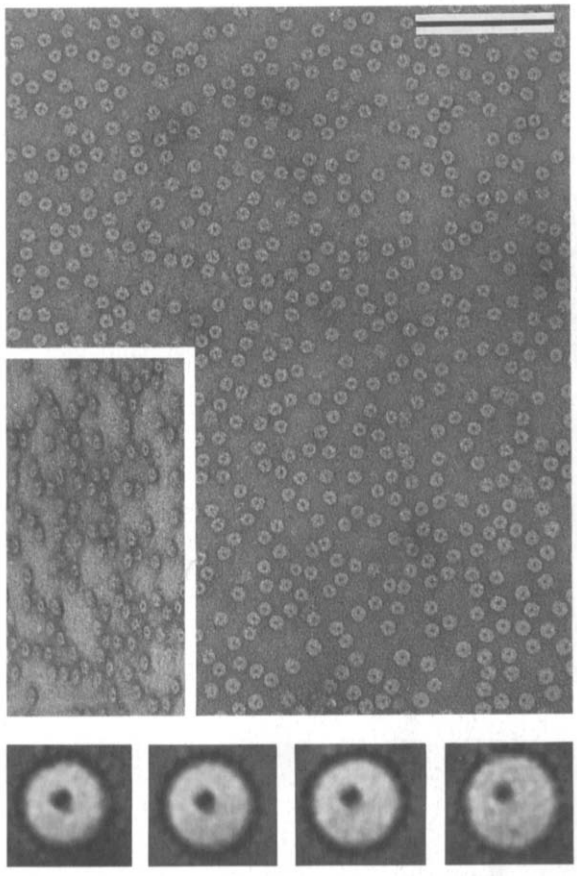

Fig.2. (a) Micrograph demonstrating the variability in dimensions and shapes encountered with uranyl acetate-stained MCP preparations. Compare particle dimensions at the top left corner and at the bottom right corner. At the bottom four averages of the major classes of molecular images as revealed by eigenvector-eigenvalue data analysis are shown. (Inset) Micrograph of a 60° tilt of a uranyl acetate-stained preparation; in this image area the particles are affected by a substantial flattening. The circular end-on views are not gradually transformed into rectangular side views upon tilting. Bar represents 100 nm.

in a simplistic way as composed of four stacked rings. Correlation averaging over 300 (AM) or 390 (NaPT) individual images reveals a much clearer and more detailed picture of this particular projection structure (figs 3 and 4). Actually, in both negative stains showing the side-on views, NaPT and AM, the particles appear more like a tripartite structure, resembling a reel, than as a stack of four (nearly) equivalent rings. Two 11 to 12 nm long and approx. 3 to 3.5 nm wide 'rods' form the short ends of the rectangles. These terminal rods appear clearly separated from the central part of the molecule by a groove filled with negative stain. In AM stained specimens (fig.3a–c) prominent stain accumulations are found at the centre of this groove, which coincides with the (putative) cylinder axis. Within each of these two terminal rods two centres of mass are clearly resolved which are arranged asymmetrically (shifted 'upwards' in fig.3a–c) with respect to the cylinder axis. The centre of the molecule is composed of two opposing non-equivalent bifurcate structures enclosing another prominent stain accumulation; it is centered on a plane which runs perpendicular to the cylinder axis and divides the molecules into two halves, indistinguishable from each other at the resolution attained (but note the asymmetric mass distribution in the central part of the molecule in fig.4).

While independent of the particular negative stain used, NaPT or AM, the outlines of the side-on views appear almost identical, many of the internal features described above for AM stained particles cannot be detected when NaPT is used for staining (fig.3d–f). This can only partly be attributed to the slightly higher resolution of the AM images (1.5 nm (AM) vs 1.8 nm NaPT: as defined by the radial correlation function criterion [21]) or to a facilitated penetration of AM into the interior of the cylinder. The latter effect may indeed account for the three prominent stain accumulations along the cylinder axis. It remained puzzling, however, that with the NaPT stained particles neither indications of mass accumulations in the terminal rods nor any distinct features in the central part of the molecule could be detected by straightforward correlation averaging; both these structural elements appeared rather blurred. We

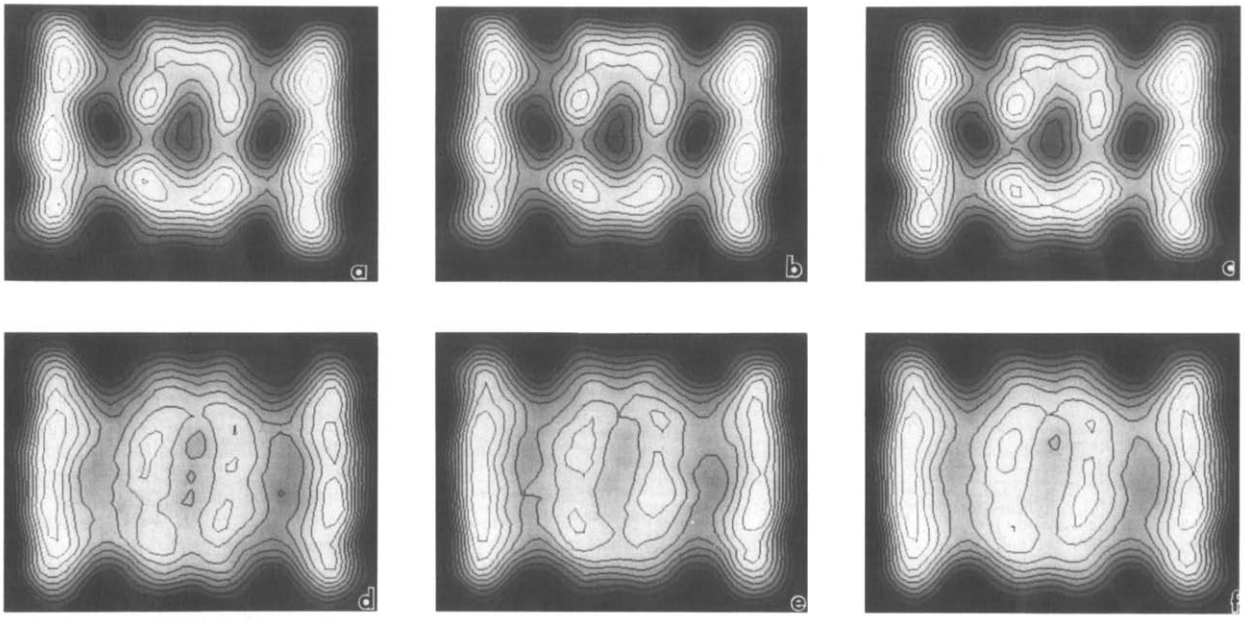

Fig.3. (a–c) Averages of side-on views of ammonium molybdate-stained MCP particles; (a,b) are independent averages over the 'even' and 'odd' members of the population, while (c) is a cumulative average over the whole population comprising approx. 300 individual images. (d–f) Averages of side-on views of sodium phosphotungstate-stained MCP particles; (c,d) 'even' and 'odd' averages, (f) cumulative average over approx. 390 individual images.

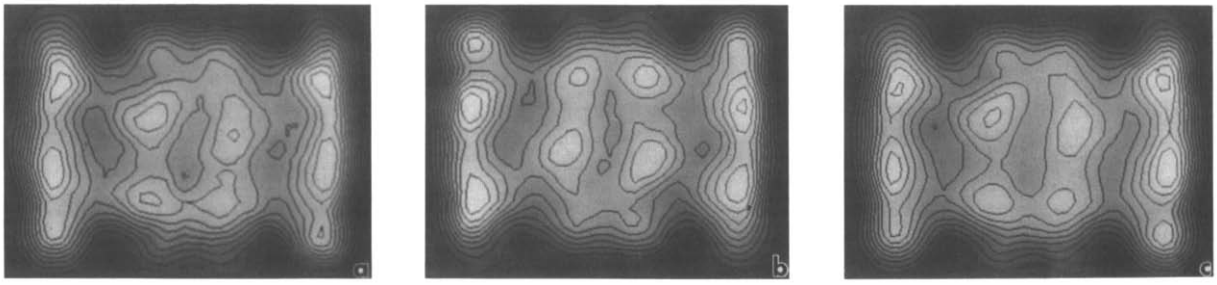

Fig.4. (a,b) Averages of the two major classes of sodium phosphotungstate-stained MCP particles obtained by eigenvector-eigenvalue data analysis showing them 'up-side up' and 'up-side down'. (c) Cumulative average of (a,b) obtained after a 180° rotation of one of them and realignment.

have therefore subjected all the 390 individual NaPT-side-on views to an image classification procedure based on eigenvector-eigenvalue analysis. As a result we obtained two classes of images which can be brought into register by a 180° rotation around the central axis running vertical to the image plane (fig.4a,b). This implies that, possibly as a consequence of the somewhat lower resolution in the NaPT data set, cross-correlation has failed to discriminate between these two orientations. Indiscriminate averaging over two about equally large populations of up-side-up and up-side-down molecules of course cancels out the particle's asymmetry and causes a blurring of features. In fig.4c we have recombined the two classes after rotating one of them by 180° and realignment. This cumulative average in fact shows the same mass disposition in the two terminal rods as observed with AM stained preparations. Also the mass disposition in the central part of the molecule now shows a closer resemblance to the situation with AM. This implies, that in both preparations the particles prefer the same orientation on the grid.

End-on projections of the MCP particles were available from three different preparations (AM, UA and ATG). Images from UA stained preparations have been excluded from further image analysis because the structure of the particles has been destabilized leading to a variability in shapes and dimensions (table 1). This, in turn, results in blurring of the averaged images shown in fig.2. Averages of AM stained particles are shown in fig.5. A comparison of the four averages shows that details of the mass disposition within the ring are subject to slight variations depending on the particular reference image chosen for the alignment in the first averaging cycle indicating a slight residual bias. In any case, however, the ring-shaped molecular images are approx. 11 nm in diameter with a stain filled center of approx. 4 nm in diameter. Within the ring six local centres of

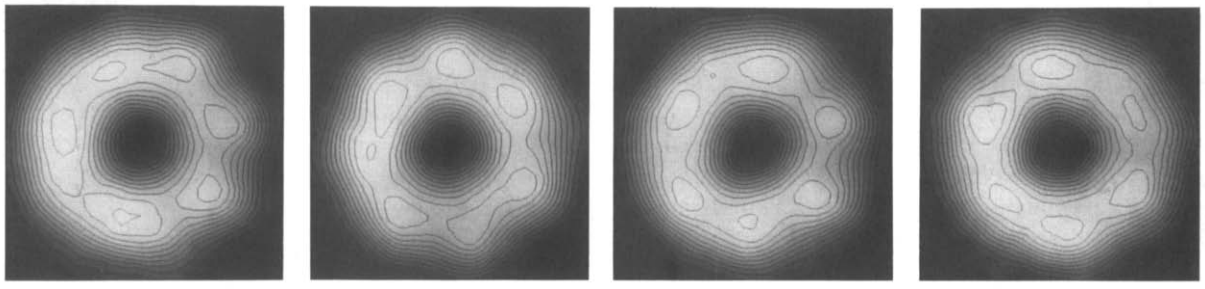

Fig.5. Four independent averages of end-on views from an ammonium molybdate-stained preparation. Different molecular images were used as a reference to assess a possible bias. In spite of minor variations we find, independent of the reference being used six local centres of mass; these appear not strictly related to each other by six-fold rotational symmetry.

mass are visible. We, however, refrained from imposing 6-fold rotational symmetry on the averages of the end-on projections because of the noticeable departure from angular increments of 60° in the positions of these mass centres.

4. DISCUSSION

Molecular complexes which appear upon visual inspection of electron micrographs as stacks of four rings or disks are quite common in nature. A large number of structures has actually been described which by the criteria of size and shape resemble the MCP particles described in this communication. In the case of the ubiquitous 19 S ribonucleoprotein (19 S-scRNP) the homology with MCP is not only suggested by this kind of morphological data, it is also strongly supported by biochemical and immunological data [10].

Another particle that has been described in the literature is the 'hollow cylinder protein' or 'cylindrin' [22]. It has a strikingly similar gross morphology, its behaviour in different stains is similar to what we observed with MCP and it has a very similar subunit composition according to SDS-polyacrylamide gels [23,24]. Although cylindrin has as yet not been tested for enzymatic activity, we believe that this molecule, a major component of erythrocytes from various sources [25] is also homologous to MCP.

Shelton et al. [26] described an 18–20 S rectangular particle, about 10 × 14.5 nm in size which occurs in the same two orientations (end-on and side-on), characteristic of the MCP; it co-purified with an aminoacyl-tRNA synthetase. Harris [25] claimed, based on morphological data, the aminoacyl-tRNA synthetase to be identical with cylindrin. Dang [27], on grounds of biochemical arguments, disputed this identity. We have examined commercial crude aminoacyl-tRNA synthetase preparations from four different sources by electron microscopy and only very rarely found particles remotely reminiscent of MCP (not shown). We tend to believe that these spurious ring shaped or rectangular structures represent only contaminants; they can certainly not be regarded as a proof of identity.

Other structures, which show at first glance a high degree of similarity with MCP include glycogen-synthase [28], groE from *E. coli* [29] or the *Bordetella pertussis* protective antigen [30]. While the dimensions of the four-stacked glycogen synthase particles differ too much, and while groE shows contrary to MCP a distinct 7-fold symmetry in end-on views making closer structural, or functional relationship unlikely, the *B. pertussis* 22 S protective antigen has not yet been subjected to a detailed structural analysis.

Kleinschmidt et al. [17] 'repeatedly observed in favourably stained particles' (2% uranyl acetate) 'that the cylinder walls' [of their 22 S cylinder particle of *Xenopus laevis* which is homologous to MCP (Wolf, D.H., personal communication)] 'were not uniform but composed by granular subunits, mostly six, that were symmetrically arranged'.

As we have shown previously [16] a drastically enlarged diameter of MCP molecules is observed with UA stained specimens when compared with conically coated freeze-dried preparations. In this communication we have presented evidence for a dramatic inter-particle variation of UA stained MCP and a substantial flattening. Because of the aberrant behaviour of MCP molecules stained with UA such images are not suitable for a reliable structural analysis. Arrigo et al. [8] have claimed the large multicatalytic proteinase to possess 8-fold radial symmetry. This is based on electron micrographs of particles stained with UA which were subjected to Markham rotation analysis [31]. This technique is based on the a priori assumption of rotational symmetry. Our analysis of end-on views does not completely rule out the existence of a rotational symmetry (which is easily violated by preparation induced artefacts) but even with the (most trustworthy) AM stained preparations our image analysis would not justify to impose any symmetry – certainly not 8-fold symmetry.

Several of the open questions regarding the molecular architecture of the MCP particle can only be settled by performing a complete 3D reconstruction.

Acknowledgements: The authors wish to thank Dr U. Aebi (Basel) for helpful discussions. This work was supported by the Deutsche Forschungsgemeinschaft (Bonn), the Ministerium für Wissenschaft und Forschung des Landes Nordrhein-Westfalen, and the Bundesministerium für Jugend, Familie, Frauen und Gesundheit (Bonn).

REFERENCES

[1] Wilk, S. and Orlowski, M. (1983) J. Neurochem. 40, 842–849.
[2] Dahlmann, B., Kuehn, L., Rutschmann, M. and Reinauer, H. (1985) Biochem. J. 228, 161–170.
[3] Tanaka, K., Ii, K., Ichihara, A., Waxman, L. and Goldberg, A.L. (1986) J. Biol. Chem. 261, 15197–15202.
[4] Dahlmann, B., Rutschmann, M., Kuehn, L. and Reinauer, H. (1985) Biochem. J. 228, 171–177.
[5] Ishiura, S., Yamamoto, T., Nojima, M. and Sugita, H. (1986) Biochim. Biophys. Acta 882, 305–310.
[6] Dahlmann, B., Kuehn, L., Kopp, F., Reinauer, H. and Stauber, W.T. (1988) in: Proteases: Potential Role in Health and Disease (Hörl, W.H. and Heidland, A. eds) Plenum, in press.
[7] Stauber, W.T., Fritz, V.K., Maltin, C.A. and Dahlmann, B. (1987) Histochem. J. 19, 594–597.
[8] Arrigo, A.P., Tanaka, K., Goldberg, A.L. and Welch, W.J. (1988) Nature 331, 192–194.
[9] Arrigo, A.P., Simon, M., Darlix, J.L. and Spahr, P.F. (1987) J. Mol. Evol. 25, 141–150.
[10] Falkenburg, P.E., Haass, C., Kloetzel, P.M., Niedel, B., Kopp, F., Kuehn, L. and Dahlmann, B. (1988) Nature 331, 190–192.
[11] Narayan, K.S. and Rounds, D.E. (1973) Nature New Biol. 243, 146–150.
[12] Harmon, F.R., Spohn, W.H., Domae, N., Ha, C.S. and Busch, H. (1983) Cell Biol. Int. Rep. 7, 333–343.
[13] Schuldt, C. and Kloetzel, P.M. (1985) Dev. Biol. 110, 65–74.
[14] Tanaka, K., Yoshimura, T., Ichihara, A., Kameyama, K. and Takagi, T. (1986) J. Biol. Chem. 262, 15204–15207.
[15] Martins de Sa, C., Grossi de Sa, M.-F., Akhayat, O., Broders, F., Scherrer, K., Horsch, A. and Schmid, H.-P. (1986) J. Mol. Biol. 187, 479–493.
[16] Kopp, F., Steiner, R., Dahlmann, B., Kuehn, L. and Reinauer, H. (1986) Biochim. Biophys. Acta 872, 253–260.
[17] Kleinschmidt, J.A., Hügle, B., Grund, C. and Franke, W.W. (1983) Eur. J. Cell Biol. 32, 143–156.
[18] Van Heel, M. and Frank, J. (1981) Ultramicroscopy 6, 187–194.
[19] Hegerl, R. and Altbauer, A. (1982) Ultramicroscopy 9, 109–116.
[20] Saxton, W.O., Pitt, T.J. and Horner, M. (1979) Ultramicroscopy 4, 343–354.
[21] Saxton, W.O. and Baumeister, W. (1982) J. Microsc. 127, 127–138.
[22] Harris, J.R. (1969) J. Mol. Biol. 46, 329–335.
[23] Harris, J.R. and Naeem, I. (1978) Biochim. Biophys. Acta 537, 495–500.
[24] Malech, H.L. and Marchesi, V.T. (1981) Biochim. Biophys. Acta 670, 385–392.
[25] Harris, J.R. (1983) Micron. Microsc. Acta 14, 193–205.
[26] Shelton, E., Kuff, E.L., Maxwell, E.S. and Harrington, J.T. (1970) J. Cell Biol. 45, 1–8.
[27] Dang, Chi V. (1984) Cell Biol. Int. Rep. 8, 323–327.
[28] Rebhun, L.I., Smith, C. and Larner, J. (1973) Mol. Cell. Biochem. 1, 55–61.
[29] Hohn, T., Hohn, B., Engel, A., Wurtz, M. and Smith, P.R. (1979) J. Mol. Biol. 129, 359–373.
[30] Sato, Y. and Nagase, K. (1967) Biochem. Biophys. Res. Commun. 27, 195–201.
[31] Horne, R.W. and Markham, R. (1972) in: Practical Methods in Electron Microscopy (Glauert, A.M. ed.) vol.1, part 2, pp.327–434, North-Holland, Amsterdam.